Supporting Information

Solar-Driven Bistable Thermochromic Textiles based on Supercooling and Space Constraint Anchoring Electron Transfer

Chengcheng Wang,[a] Jingwen Wang,[a] Liping Zhang,*[a] and Shaohai Fu[a]

[a] Jiangsu Engineering Research Center for Digital Textile Inkjet Printing, Key Laboratory of Eco-Textile, Jiangnan University, Ministry of Education, Wuxi, Jiangsu 214122, China.

*E-mail: zhanglp@jiangnan.edu.cn

1. Supplementary Methods: Materials & Characterization

2. Supplementary Figures: Figure S1-20

3. Supplementary Table: Table S1

Supplementary methods

1. Materials

Hexadecanol ($C_{16}OH$, 98 %), Diphenyl carbonate (DPC, 99 %), glyceryl monostearate (GM, 98 %), glyceryl distearate (GD, 98 %), polyethylene glycol cetyl ether (PGCE, 99 %), Nano silicon carbide (Nano SiC) were purchased from MACKLIN. Bisphenol A (BPA), Arabian gum powder, Urea, Formaldehyde, Melamine, Glacial acetic acid, Sodium hydroxide were obtained from Sinopharm Chemical Reagent Co., Ltd., China. 4'-(benzyloxy) phenethyl decanoate (BPD, 98 %) was supplied by Wuhan Lu Hao New Material Co. Ltd. 6'-(Diethylamino)-1',3'-dimethylfluorane (DDF, orange), 2'-chloro-6' - (diethylamino) fluorane (red), 3',6'-dimethoxyfluorane (yellow), Crystal violet lactone (blue), 6'-(diethylamino)-2'-(phenylamino)-3H-spiro[isobenzofuran-1,9'-xanthen]-3-one (dark green), 3,3-bis(2-ethoxy-4-N,N-diethylaMinophenyl)-7(4)-azaphthalide (aqua) were purchased from Wuhan Hai Shan Technology Co., Ltd., China. Thickener and Binder were purchased from Hefei Hua Yue New Material Technology Co., Ltd, China. All above reagents were used without further purification unless otherwise mentioned.

2. Characterization

The apparent morphology and optical properties of SDBTC-Ms and SDBTCT were observed by scanning electron microscopy (SEM, SU1510, Hitachi, Co., Ltd, Japan) and optical microscope (OM; DM2700P, Leica Microsystems Co., Ltd., Germany). The structures of BTC, BTC-Ms (without nano SiC) and SDBTC-Ms were determined using Attenuated Total internal Reflectance Fourier Transform Infrared (ATR-FTIR) spectrometer (Nicolet is 10, Thermo Nicolet Co., Ltd, USA). Energy-dispersive X-ray spectroscopy (EDAX, Elect Plus, Ametek USA) was used to determine the elemental composition, element mapping, and content of the materials of SDBTC-Ms. Thermal analysis of BTC and SDBTC-Ms were measured by differential scanning calorimetry (DSC; Q-200, TA Instruments, USA), which was carried out with a heating and cooling speed of 5 ^{o}C/min. Thermogravimetric analysis (TGA, Q-500, TA Instruments, USA) was used to investigate thermal degradation of samples in the temperature form 0 ^{o}C to 600 ^{o}C at a heating rate of 10 ^{o}C/min under a flow of nitrogen. Reflectance spectra of SDBTC-Ms and SDBTCT was observed and recorded via Fiber-optical spectrometer (FOS, FX-2000, Idea-Optic Co., Ltd, China) and computer color matching instrument (Data color DC850, America) with the temperature change. Thermal infrared imager (testo 871, Germany) was used to minor the temperature change in simulated sunlight.

3 Fastness properties

To evaluate the actual wearability of SDBTCT, a series of fastness tests, such as washing, friction, and durability, were carried out and analyzed. As shown in Fig. S17a, SDBTCTs have no obvious fading and staining after the wash test. Furthermore, SDBTCT retains color-change and bistability after wash and friction fastness tests and has the same color depth at both ST I and ST II as the original SDBTCT (Fig. S17b-f).

To further explore the durability of SDBTCT, its color-change performance and bistability were studied and recorded after a series of repeated actions including light on and off, heating and cooling. Fig. S17g-i show that the color of SDBTCT is still maintained after 140 repeated light on and light off (or heating and cooling) cycles, and both ST I and ST II still exist, indicating good durability in both solar-driven thermochromic performance and bistability.

Supplementary Figures

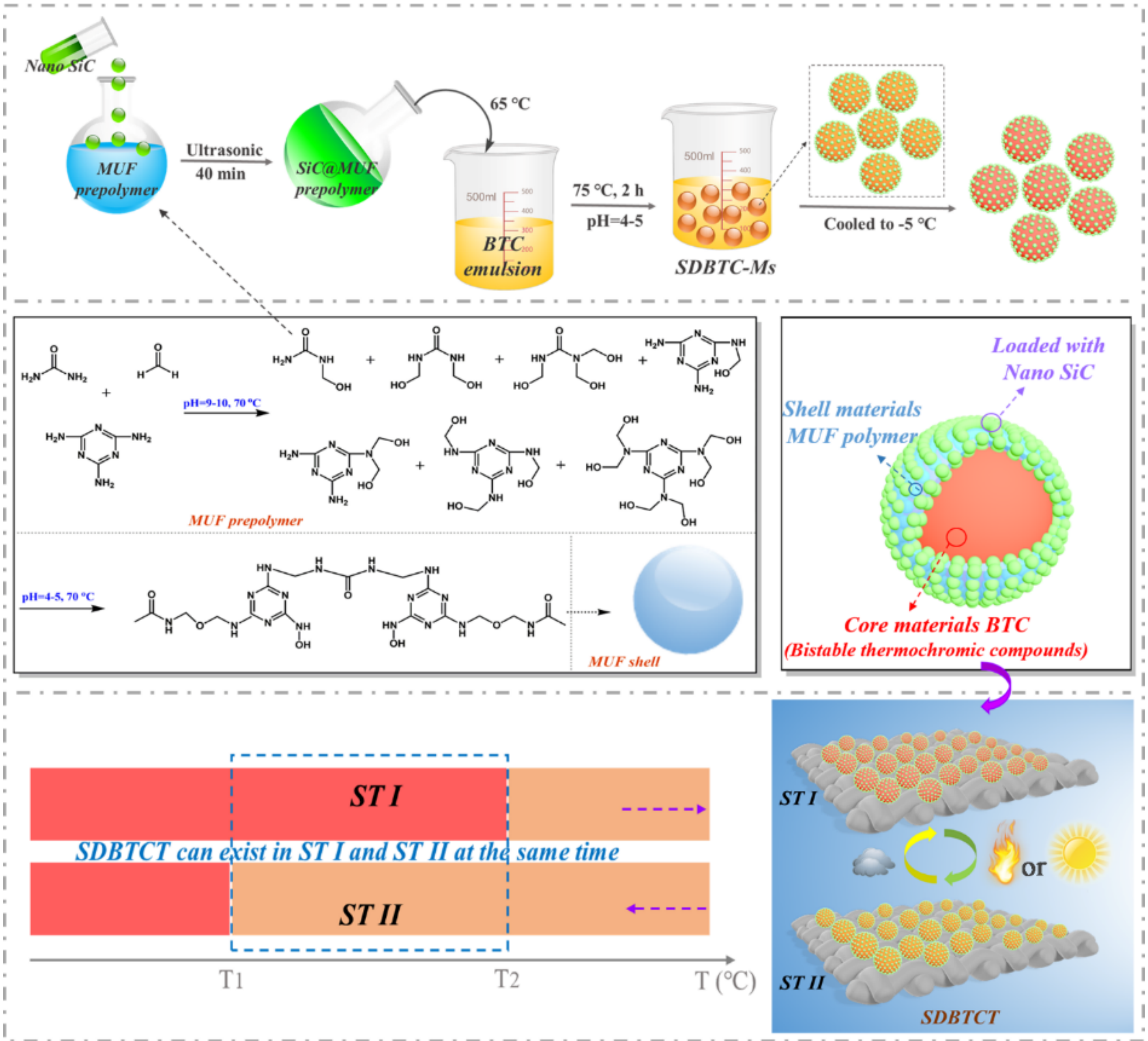

Fig. S1 Schematic diagram of the preparation process and bistable property of SDBTC-Ms.

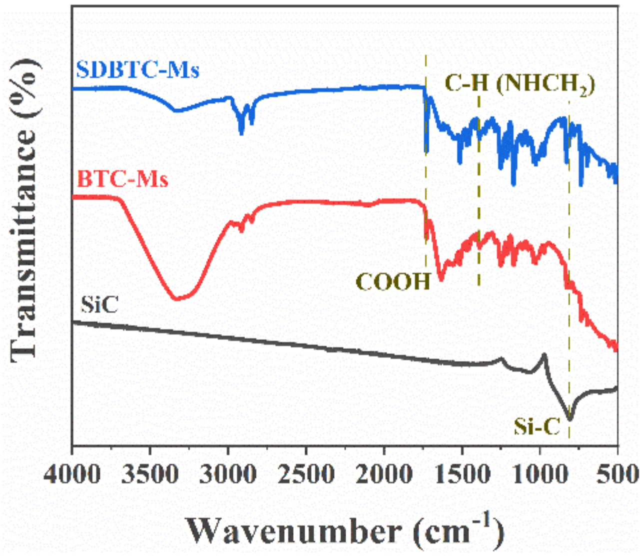

Fig. S2 FT-IR spectra of SiC, BTC-Ms and SDBTC-Ms.

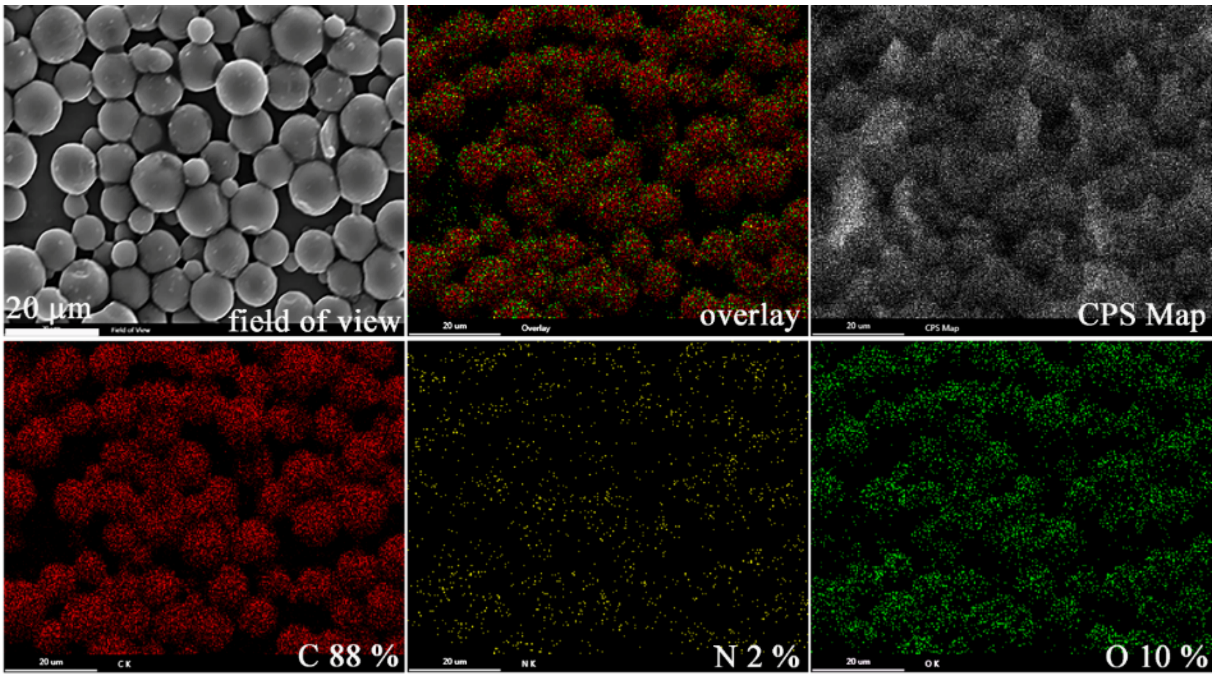

Fig. S3 SEM-EDS mapping images of bistable thermochromic microcapsules without nano SiC.

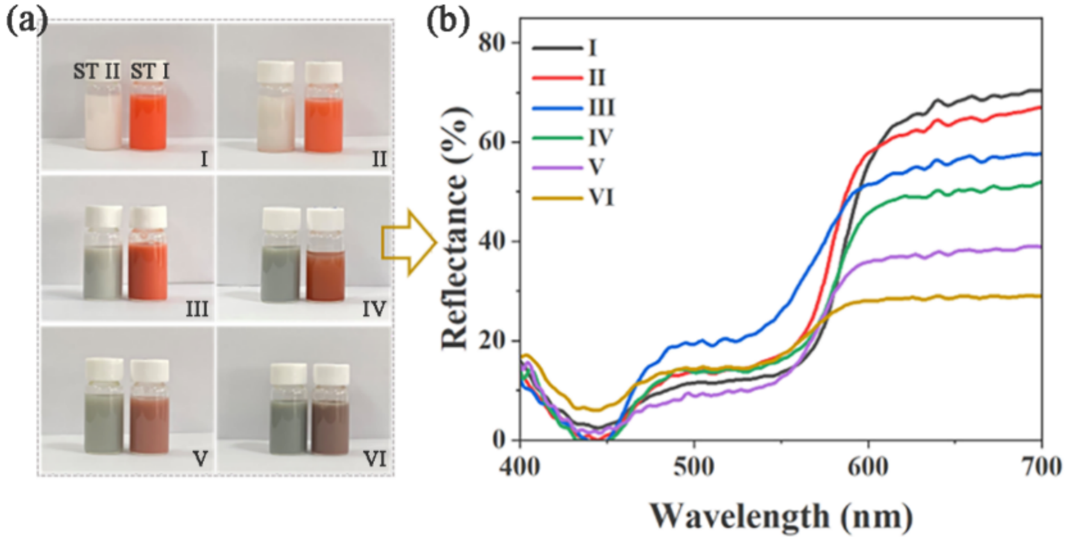

Fig. S4 (a) Digital photos of SDBTC-Ms dispersion (I to VI, nano SiC content: 0 %, 0.5 %, 1 %, 3 %, 5 % and 7 % respectively). (b) Reflectance spectra of SDBTC-Ms in ST I.

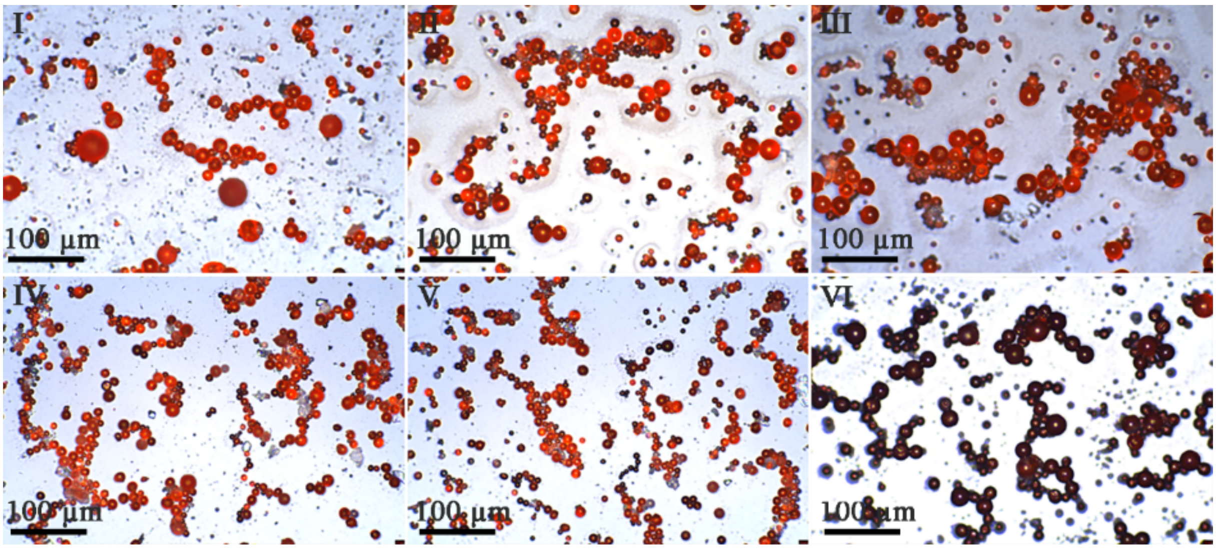

Fig. S5 Optical microscope (OM) images of SDBTC-Ms (I to VI, experimental nano SiC material ratio is 0 %, 0.5 %, 1 %, 3 %, 5 % and 7 % respectively).

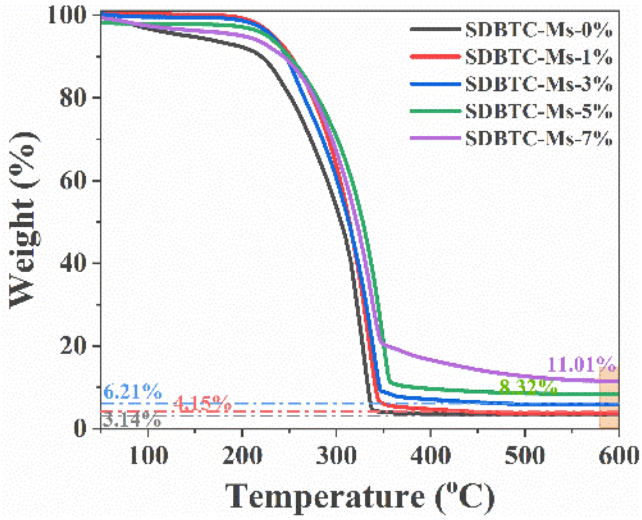

Fig. S6 TG curves of SDBTC-Ms with different contents of nano SiC.

Thermal decomposition analysis of SDBTC-Ms with different nano SiC contents was used to determine whether polymeric structures retain the same amount of SiC. Nano SiC do not decompose before 600 °C. Therefore, carbon yield ratio of SDBTC-Ms at 600 °C insists of microcapsules after thermal decomposition and undecomposed SiC. The real amount of SiC can be defined as the difference between the carbon yield ratio of SDBTC-Ms-x % and that of SDBTC-Ms-0 %. Results shows that the resulting polymeric structures retain the same amount of SiC.

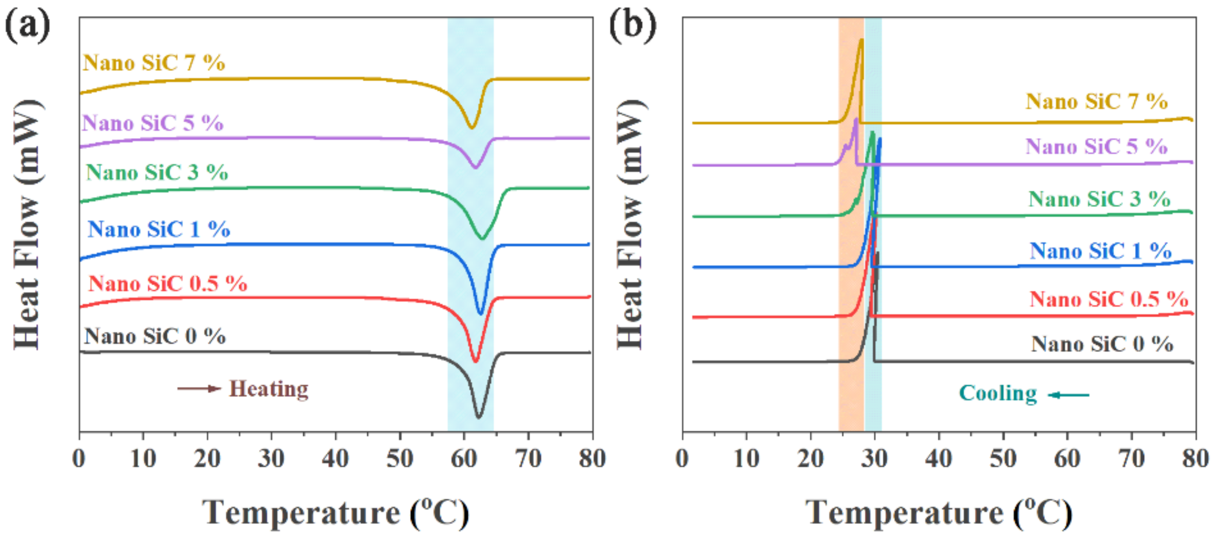

Fig. S7 DSC curves of SDBTC-Ms.

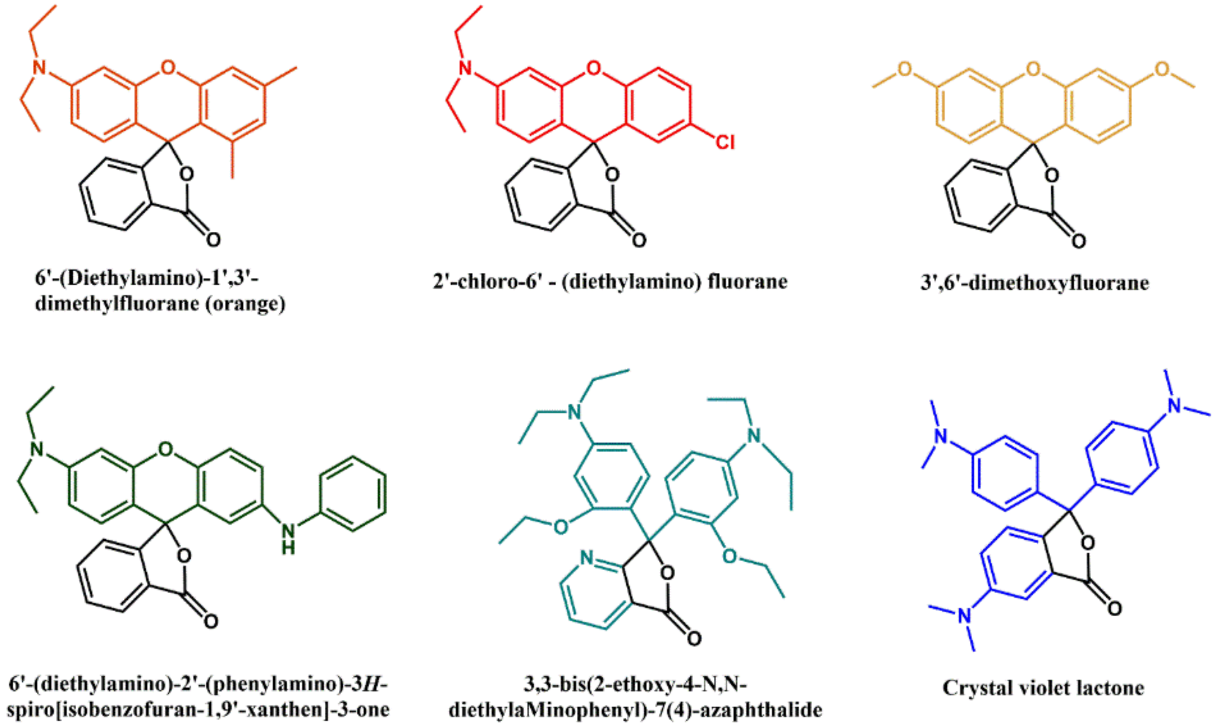

Fig. S8 Structures for fluorane dyes which were selected to adjust color.

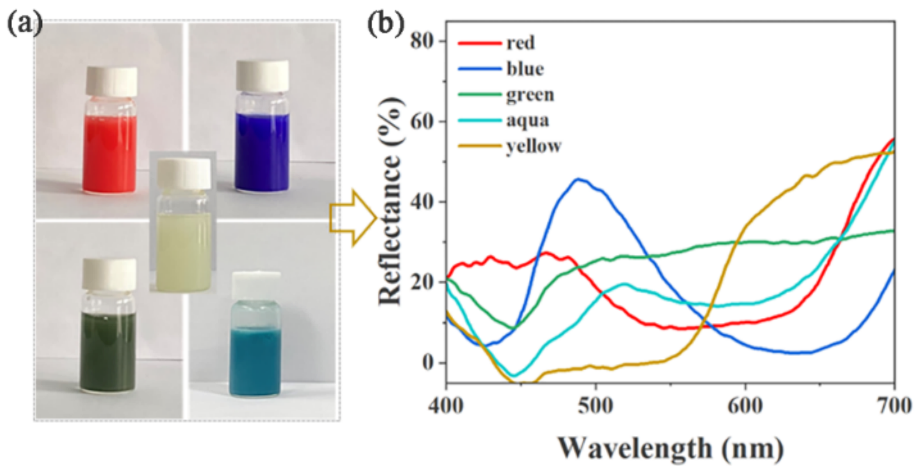

Fig. S9 Digital photos (a) and reflectance spectra (b) of the colorful SDBTC-Ms in ST I.

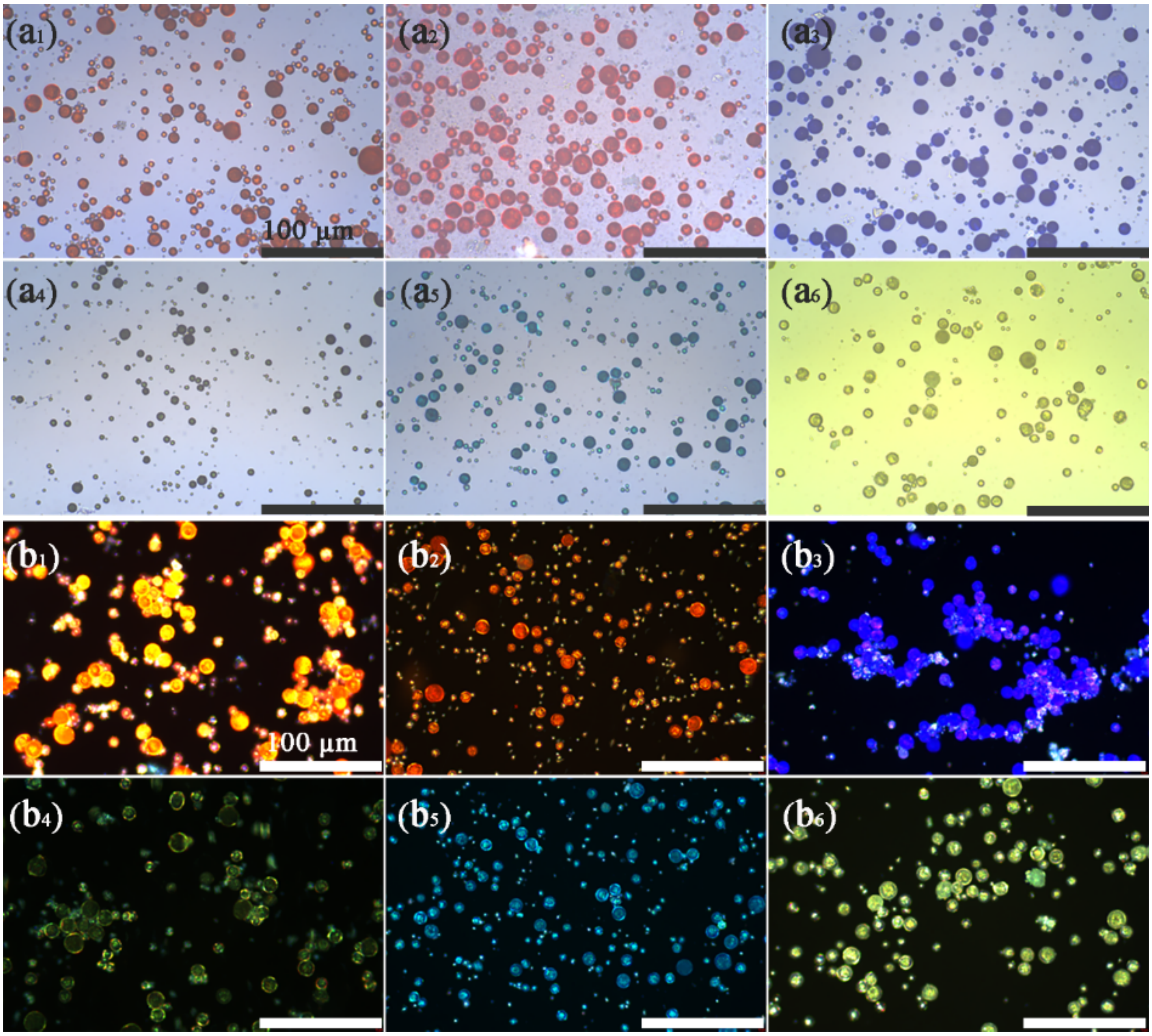

Fig. S10 OM images (a) and PM image (b) of colorful SDBTC-Ms: (a_1-a_6, b_1-b_6) are orange, red, blue, dark green, aqua and yellow in turn.

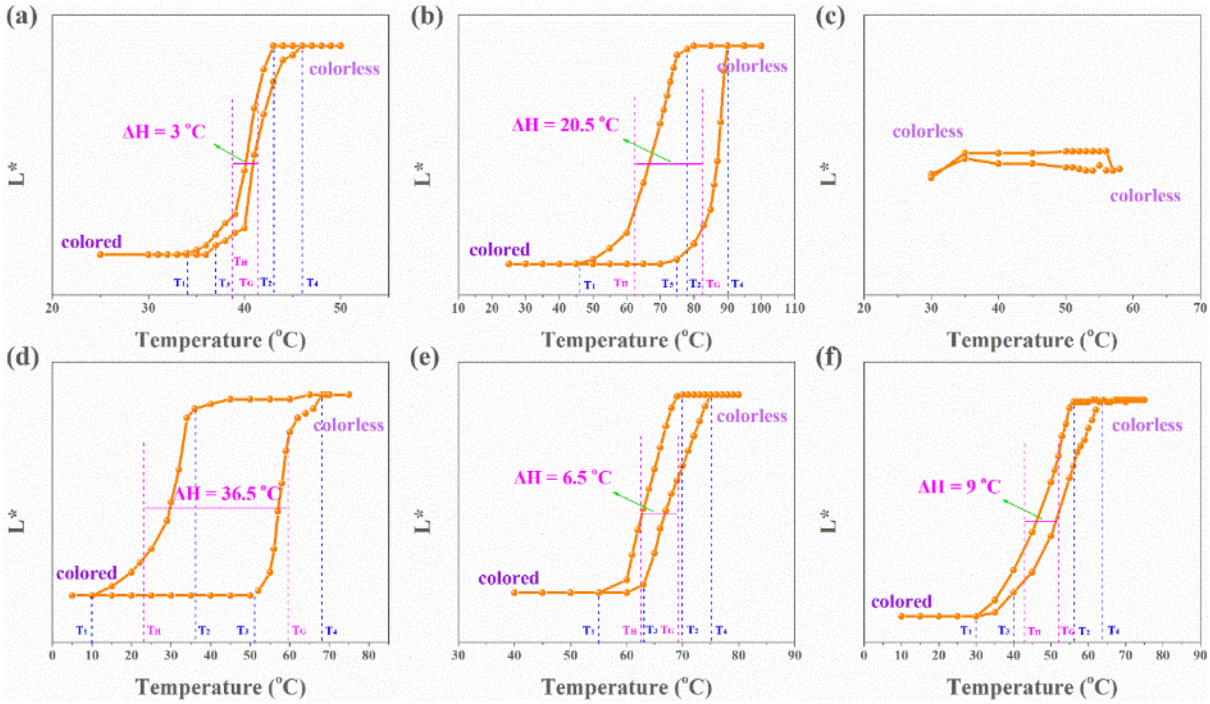

Fig. S11 Thermochromic performance of BTC with different PCMs. (a) $C_{16}OH$, (b) DPC, (c) PGCE, (d) BPD, (e) GM, and (f) GD.

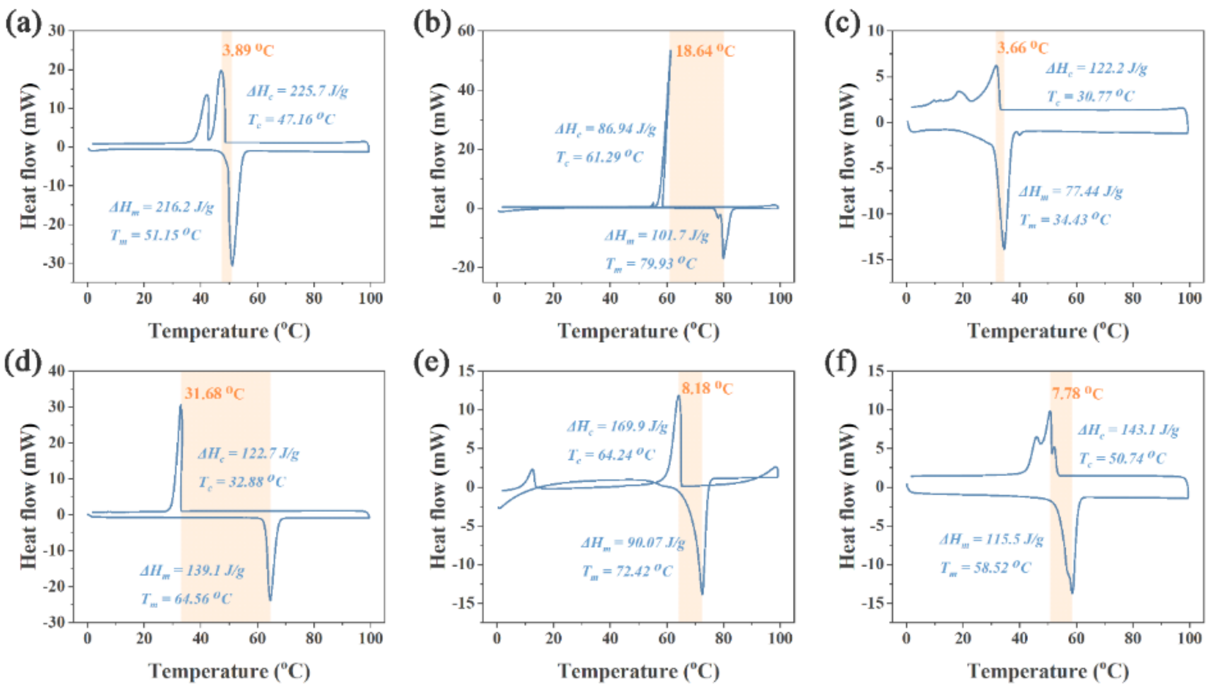

Fig. S12 DSC curves of (a) $C_{16}OH$, (b) DPC, (c) PGCE, (d) BPD, (e) GM, and (f) GD.

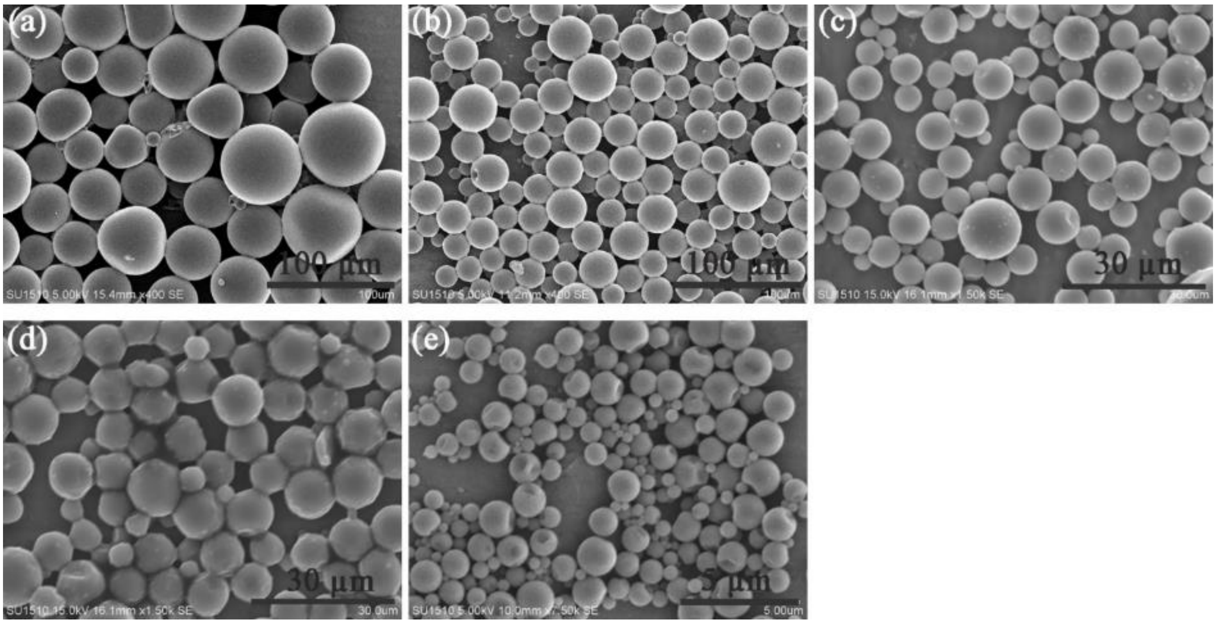

Fig. S13 SEM images of SDBTC-Ms prepared with different emulsification rate. (a) 1000 rpm. (b) 2000 rpm. (c) 6000 rpm. (d) 8000 rpm. (e) 10000 rpm.

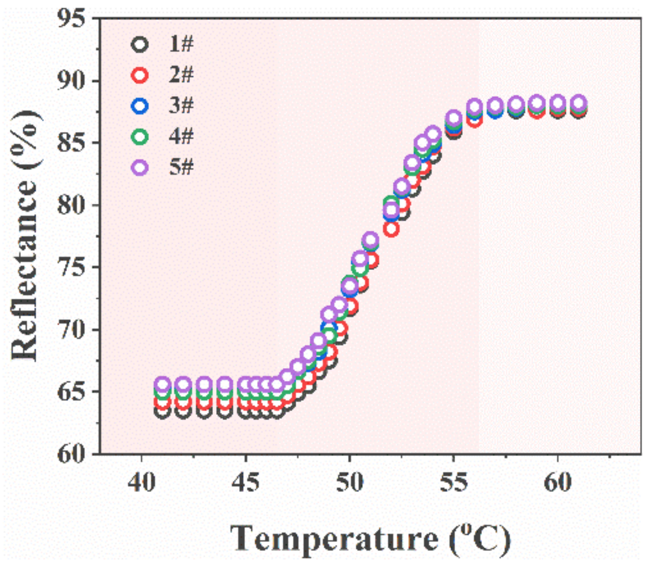

Fig. S14 Reflectance changes of BTC-Ms in the cooling process (reflectance test at 600 nm; mean particle size: 1#: 45 μm, 2#: 30 μm, 3#: 10 μm, 4#: 5 μm, 5#: 1 μm).

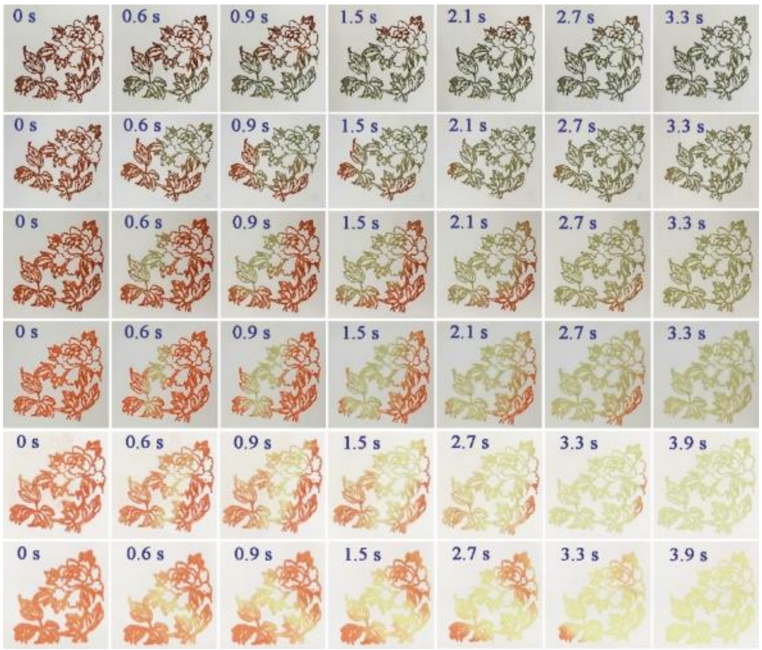

Fig. S15 Thermochromic behavior of the SDBTCT prepared using BTC-Ms with different contents of nano SiC (from the bottom of, I: 0 %, II: 0.5 %, III: 1 %, IV: 3 %, V: 5 %, VI: 7 %).

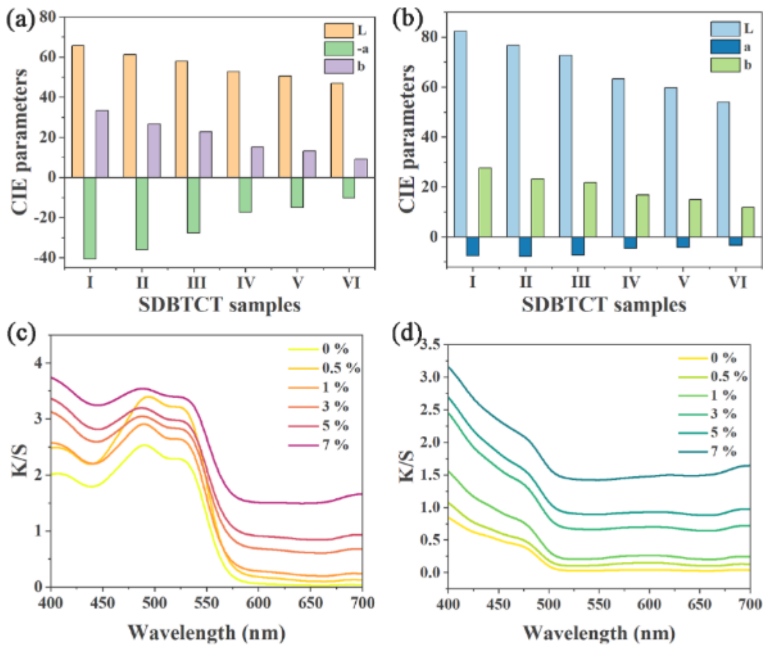

Fig. S16 CIE L*, a, b value of SDBTCT at (a) ST I, and (b) ST II. SDBTCT were prepared using BTC-Ms with different contents of nano SiC (I: 0 %, II: 0.5 %, III: 1 %, IV: 3 %, V: 5 %, VI: 7 %) (nano SiC content: I: 0 %, II: 0.5 %, III: 1 %, IV: 3 %, V: 5 %, VI: 7 %). Color depth of SDBTCT at (c) ST I, and (d) ST II

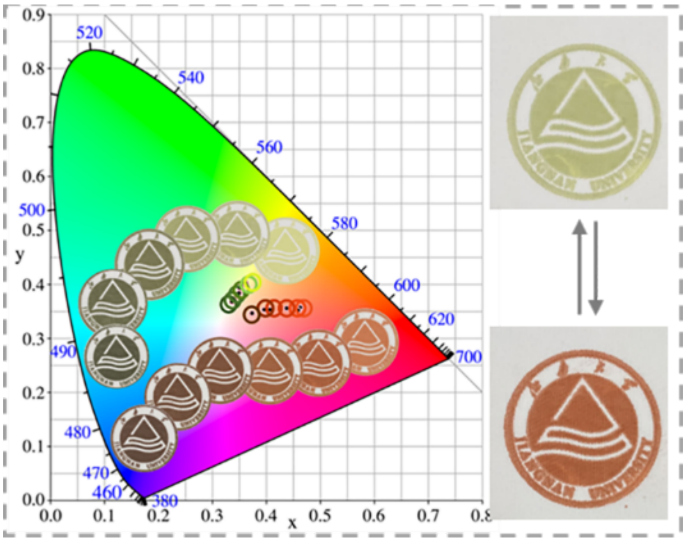

Fig. S17 CIE 1931 chromaticity diagram and optical photos of SDBTCT prepared using BTC-Ms with different contents of nano SiC (from right to left, I: 0 %, II: 0.5 %, III: 1 %, IV: 3 %, V: 5 %, VI: 7 %).

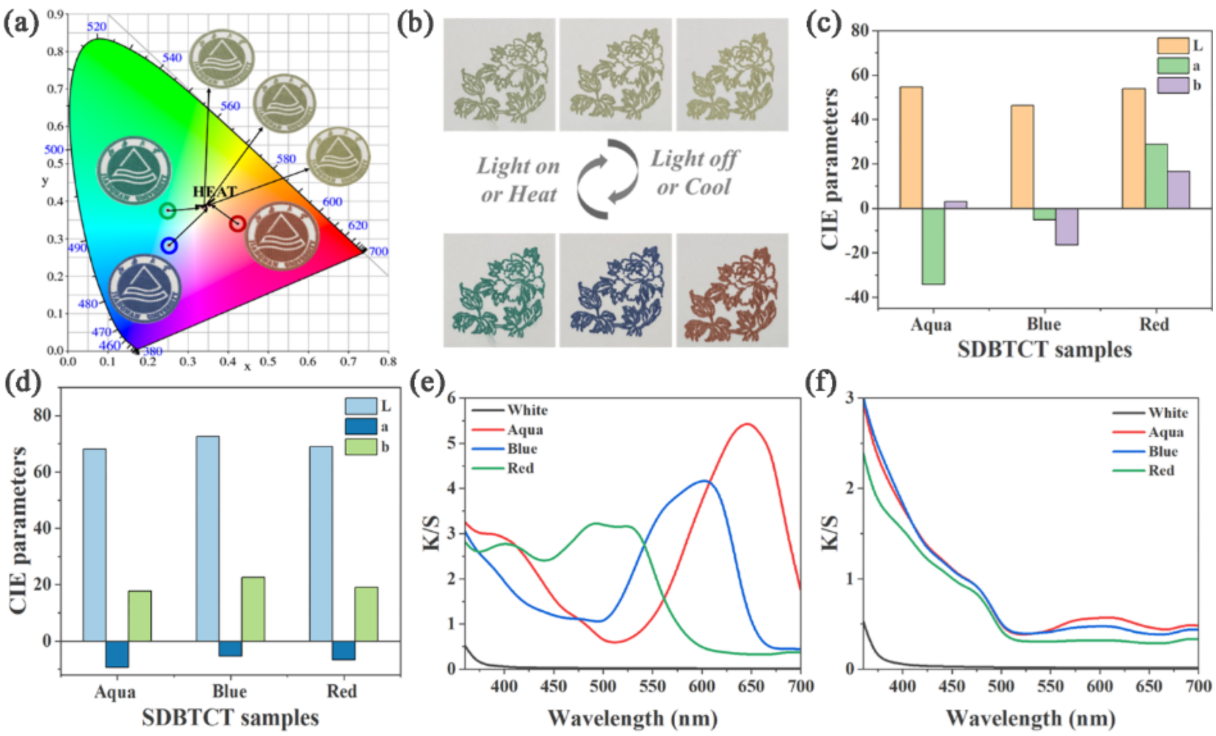

Fig. S18 Color performance of aqua, blue, and red SDBTCT. (a) The CIE 1931 chromaticity diagram and optical photos of SDBTCT. (b) Digital photos of SDBTCT. CIE L*, a, b value of SDBTCT in (c) ST I, and (d) ST II. The color depth of SDBTCT in (e) ST I, and (f) ST II.

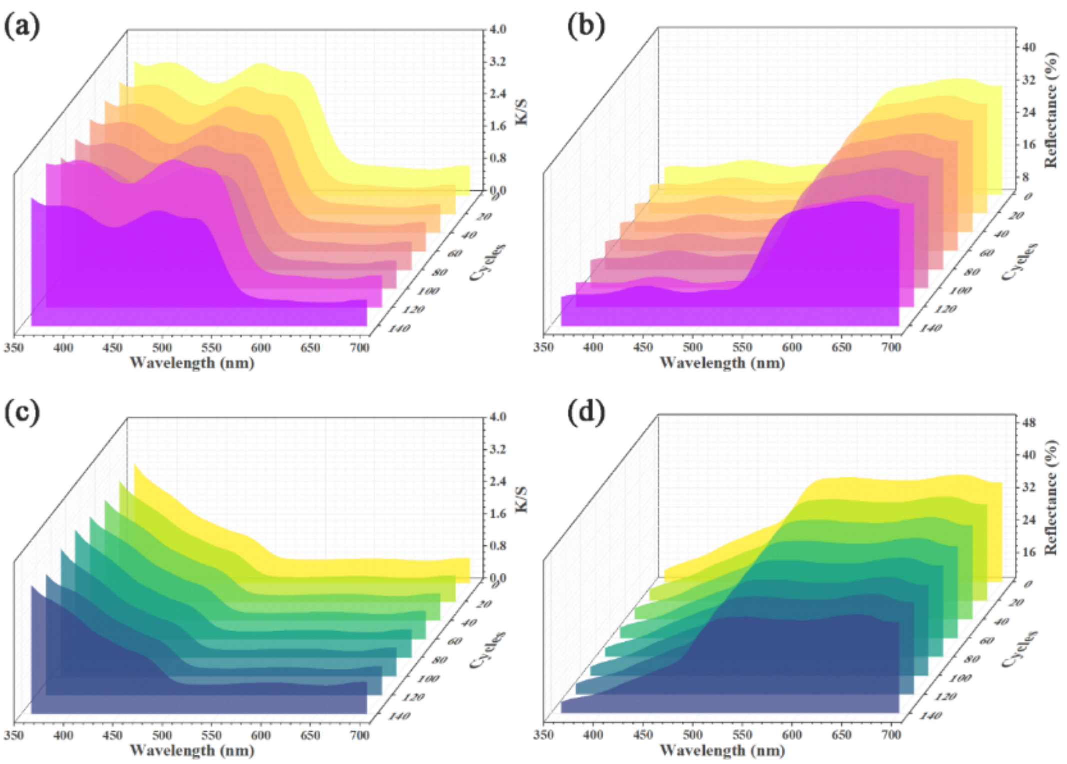

Fig. S19 Cycling performance. (a) K/S curves, and (b) Reflectance spectra of SDBTCT prepared with 3 % nano SiC BTC-Ms at ST I. (c) K/S curves, and (d) Reflectance spectra of SDBTCT prepared with 3 % nano SiC BTC-Ms at ST II.

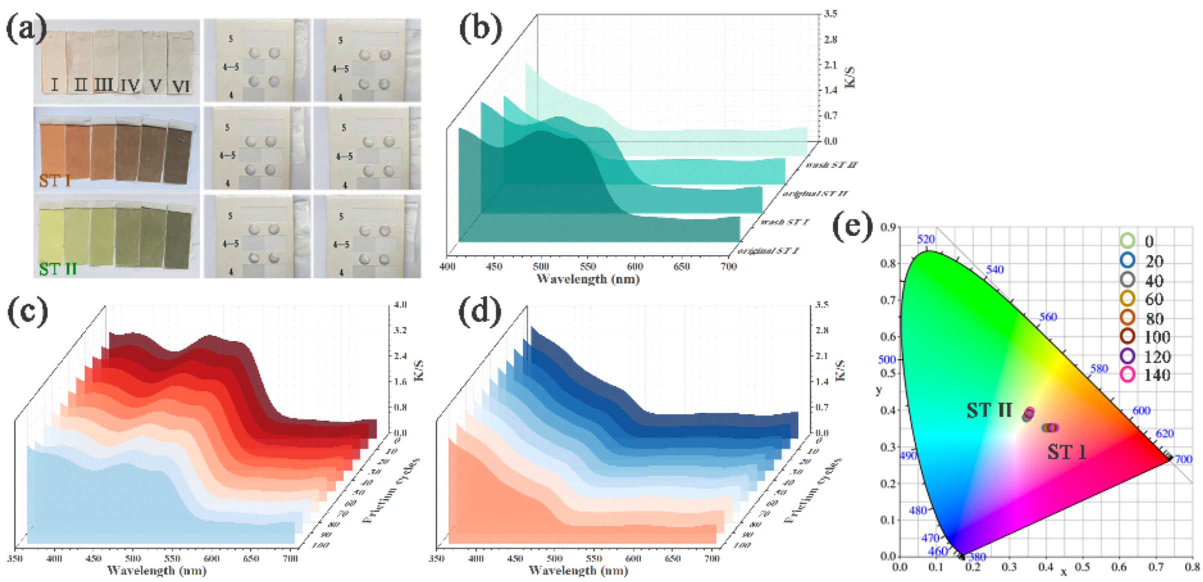

Fig. S20 Fastness test including washing, friction. (a) SDBTCT after washing test (GB/T3921-2008) digital photos (left) and gray scale for staining (right). SDBTCT were prepared using BTC-Ms with different contents of nano SiC (I: 0 %, II: 0.5 %, III: 1 %, IV: 3 %, V: 5 %, VI: 7 %). (b) Color depth of SDBTCT-IV before and after washing test. Friction test of SDBTCT-IV at ST I (c) and ST II (d) respectively. (e) The CIE 1931 chromaticity diagram of the SDBTCT-IV over 100 repeated heating-cooling cycles after washing test.

Supplementary Table

Table S1. Thermal properties of solar-driven bistable thermochromic systems.

Solid organic solvent	T_i (°C)	T_m (°C)	ΔH_m (J/g)	C_{ps} (J/(g·°C)
$C_{16}OH$	0	51.15	216.2	1.03
DPC	0	79.93	101.7	1.07
Polyethylene glycol cetyl ether	0	34.43	77.44	1.69
Decanoic acid	0	64.56	139.1	2.01
Glyceryl monostearate	0	72.42	90.07	0.38
Glyceryl distearate	0	58.52	115.5	1.14

Note: T_i, Onset temperature on DSC melting curve; T_m, Phase transition temperature on DSC melting curve; ΔH_m, Enthalpy on DSC heating curve; C_{ps}, Specific heat capacity at 25 °C.